

## CONTACT STRESSES IN GEAR TEETH DUE TO TIP RELIEF PROFILE MODIFICATION

Kristina MARKOVIĆ – Marina FRANULOVIĆ

**Abstract:** In this paper the linear tip relief profile modification has been observed. This kind of modification has been considered to be potentially dangerous considering micro-pitting initiation as a consequence of contact pressure increase. The amount of tip relief profile modification depends on the elastic gear tooth deflection that needs to be compensated. The standard gear model without linear tip relief profile modification, as well as the modified one, has been discretized by finite elements and analyzed using the finite element method to compare Hertz contact stresses on tooth flank, as influenced by the mentioned profile modification.

**Keywords:**

- spur involute gears
- profile modification
- tip relief
- FEM

### 1. INTRODUCTION

The gears' load-carrying calculation procedure is based on the assumption that gear's teeth are rigid and produced with perfect geometry. When loaded, these teeth experience deflection, both at the base of the teeth and on the tooth flank. These deflections cause modification in the relative motion of teeth flanks in opposition to the ideal one and consequently generate transmission error. Tip relief profile modification is most commonly designed to equalize with the expected deflections on the tooth tip. Therefore, transmission errors caused by these deflections are expected to be reduced by using this modification. The main reason for tip relief

modification is the appearance of so-called contact shocks during meshing, when double-teeth contact changes to single-teeth contact and vice versa. These impacts produce noise, amplify inaccuracies in the pitch, and cause deformation of the teeth under load. In order to reduce the impact influence, particularly for high loaded gears, the involute in the tip region is modified through a relief curve [1].

### 2. LINEAR TIP RELIEF PROFILE MODIFICATION

Tip relief profile modification can be designed in a few different ways. In this paper, linear tip relief modification has been considered (Figure 1).

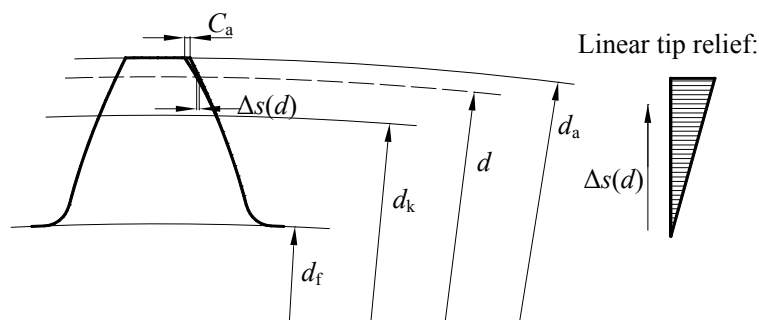


Figure 1. Linear tip relief profile modification

Tip relief profile modification is defined as the thickness  $\Delta s(d)$  of the material removed along the tooth flank with reference to the nominal involute profile.

Tooth tip diameter  $d_a$ , profile relief at tooth tip  $C_a$  and diameter at the beginning of correction  $d_k$  have to be calculated to define changes in tooth thickness (1).

$$\Delta s(d) = C_a \frac{d - d_k}{d_a - d_k} \quad (1)$$

### 3. TIP RELIEF CALCULATION FOR NOMINAL LOAD

Profile relief at tooth tip  $C_a$  is obtained as the sum of the elastic deflection of the spur gear tooth, caused by distributed load on teeth and deformation caused by Hertzian contact pressure. The diameter at the beginning of correction  $d_k$  has been found at the characteristic point B of the tooth flank.

#### 3.1. Elastic tooth deflection of the spur gear

Elastic tooth deflection caused by nominal transverse load in the plane of action is shown in Figure 2.

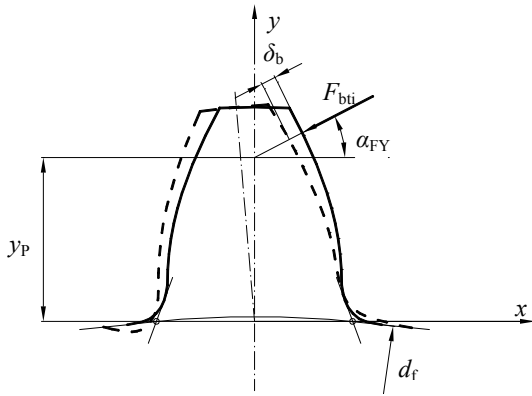


Figure 2. Elastic tooth deflection of the spur gear

Elastic tooth deflection caused by nominal transverse load has been calculated using simplified expressions [2, 3]:

$$\delta_{b1,2} = \frac{F_{bti}}{b} \frac{(1-\nu^2)}{E} \left( A + B e^{C \cdot \bar{y}_p} + D \right) \quad (2)$$

Where:

$$A = -1.05 + 153 e^{-8.1x} z^{-(1.75-1.6x)} \quad (3)$$

$$B = 0.63 + (7.35 - 0.924x) z^{-1} \quad (4)$$

$$C = 1.28 - (2.88 + 3.68x) z^{-1} \quad (5)$$

$$D = -1.06 + 0.638 \ln(m_n z) \quad (6)$$

$$\bar{y}_p = \frac{y_p}{m_n} = \frac{[r_p \cos(\alpha_b - \omega_b) - r_f]}{m_n} \quad (7)$$

$$\alpha_b = \arctan\left(\frac{\rho}{r_b}\right) \quad (8)$$

$$r_p = \frac{r_b}{\cos \alpha_b} \quad (9)$$

$$r_b = \frac{mz}{2} - m(1.25 - x) \quad (10)$$

$$\omega_b = \frac{\rho}{r_b} - \phi \quad (11)$$

$$\phi = \frac{(\pi + 4x \tan \alpha_n)}{2z} + \text{inv} \alpha_n \quad (12)$$

$$r_f = \frac{m_n z}{2} \cos \alpha_n \quad (13)$$

$$\text{inv} \alpha_n = \tan \alpha_n - \alpha_n \quad (14)$$

#### 3.2. Deformation caused by Hertzian contact stress

Hertzian contact stress refers to the localized stresses that develop as two curved surfaces come in contact and deform slightly under the imposed loads. This deformation is dependent on the elasticity of the material in contact. The Hertzian theory assumes elliptic stress distribution, with the deformed width value  $2b_H$ , as shown in Figure 3. Maximum deformation is calculated in the center of the contact area, by using equation [2]:

$$\delta_{H1,2} = \frac{2F_{bti}}{\pi b} \frac{(1-\nu^2)}{E} \left( 1.27 + 0.781 \ln \frac{m_n}{b_H} \right) \quad (15)$$

#### 3.3. Relief at tooth tip

Profile modification should be calculated for each tooth flank of the mating gears. The maximum values of the profile relief at the tooth tip of each gear are equal to the sum of elastic tooth deflection and deformation caused by Hertzian contact stress [1, 2, 3], thus it stands that:

$$C_{a1,2} = \delta_{1,2} = \delta_{b1,2} + \frac{1}{2} \delta_{H1,2} \quad (16)$$

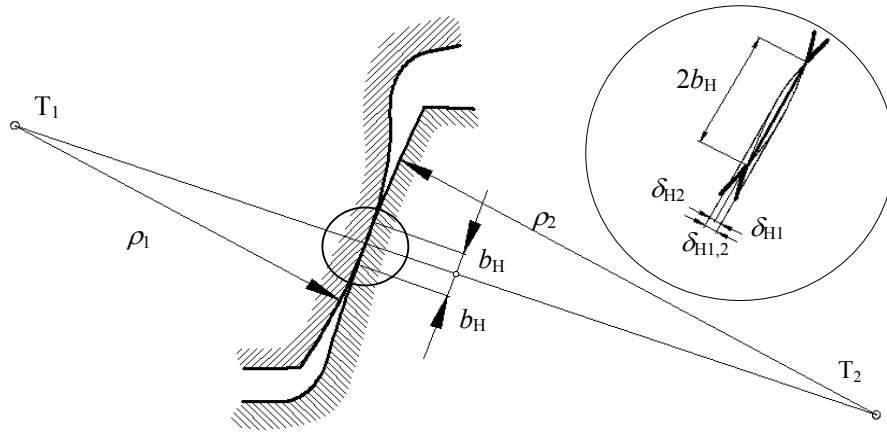


Figure 3. Deformation caused by Hertzian contact stress

### 4. SPUR GEAR CONTACT

During operation, meshed gears' teeth flanks are submitted to high contact pressures and the combination of rolling and sliding. Due to the nature of such loading, damage on the teeth flanks, in addition to tooth breakage at the tooth root, is one of the most frequent causes of gear failure.

ISO 6336 standard [4] specifies the fundamental formulae for Hertzian contact stress calculations for spur gears.

Gears teeth flanks contact can be approximated by the contact of two parallel cylinders (Figure 4) with radii equal to the radii of the curvatures of teeth flanks at the contact point.

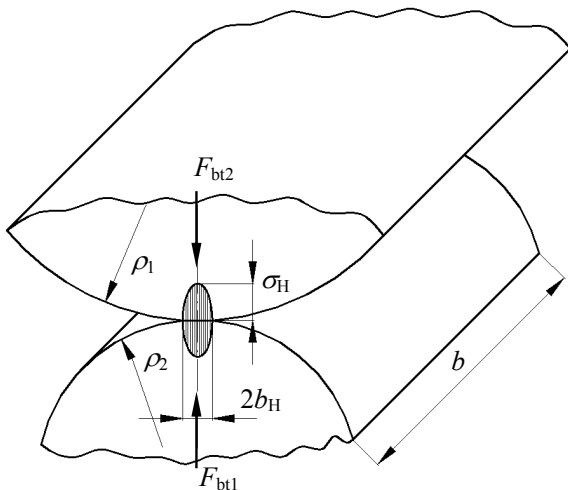


Figure 4. Parallel cylinders contact

In order to calculate contact stresses in gears, the equivalent radius of the system, maximum Hertzian

contact stress and half of the Hertzian contact width for two parallel cylinders have to be found [4]:

$$\delta_{ekv} = \frac{\delta_1 \delta_2}{\delta_1 + \delta_2} \quad (17)$$

$$\sigma_H = \sqrt{\frac{F_{bti} E}{2\pi \rho_{ekv} b}} \quad (18)$$

$$b_H = \sqrt{\frac{2F_{bti} \rho_{ekv}}{\pi b E}} \quad (19)$$

Nominal contact stress at the pitch point (stress induced in flawless gearing by application of static nominal torque) is then given by the expression [4]:

$$\sigma_{H0} = \sqrt{\frac{1}{2\pi} \frac{u+1}{u} \frac{F_{bti} E}{b d_1} \frac{2}{\cos \alpha_t \tan \alpha_{wt}}} \quad (20)$$

### 5. GEAR PAIR MODEL

A gear pair with following geometrical parameters is analyzed in this paper:

number of teeth	$z_{1,2} = 58/67$
profile shift correction	$x_{1,2} = 0$
normal module	$m_n = 12 \text{ mm}$
normal pressure angle	$\alpha_n = 20^\circ$
gear facewidth	$b_{1,2} = 330 \text{ mm}$
tool addendum factors	$h_{a^*_{01,2}} = 1.25$
bottom clearance factors	$c_{a^*_{1,2}} = 0.25$
tool tip radius factors	$\rho_{a^*_{01,2}} = 0.25$
transverse contact ratio	$\epsilon_\alpha = 1.79$

Material assigned to both gears is steel with the following material parameters:

Modulus of elasticity  $E = 210000 \text{ N/mm}^2$

Poisson's ratio  $\nu = 0.3$

According to the theoretical background for tip relief profile modification,  $C_a$  and  $d_k$  have been calculated as:

relief at tooth tip  $C_{a1,2} = 0.061/0.061$  mm  
 diameter at the beginning of correction  $d_{k1,2} = 349.223/403.358$  mm

## 6. NUMERICAL ANALYSIS

The finite element nonlinear contact analysis was chosen for modeling and simulation of the gear pair in mesh.

The analysis has been carried out by using the software package ANSYS 10.0 [5]. Newton-Raphson's method [6] has been used for the convergence of the results for this nonlinear analysis.

The load has been applied by putting in contact pinions' and wheels' teeth and applying the torsion moment on the pinion.

The gear models have been discretized by 2D finite elements that are adequate for the contact analysis.

### 6.1. Geometrical model of gears

Modeling of the entire gears in mesh would significantly increase the complexity and size of the geometric and numerical model which would, in turn, result in prolonged calculation time. Thus, already in the modeling phase certain simplifications have been made. Only segments of the hubs of the wheel and the pinion have been modeled (Figure 5), both with two whole teeth and two teeth segments [7].

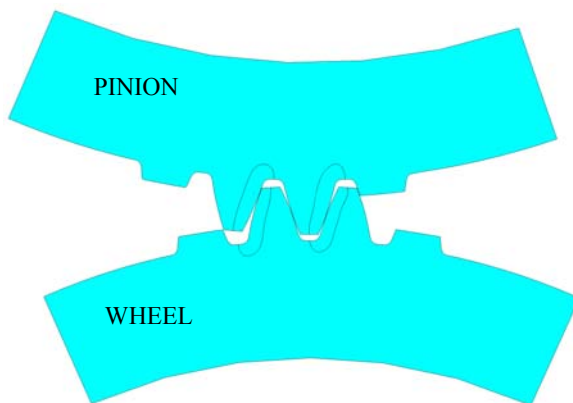


Figure 5. Geometry of gears in mesh

The distance between the root circle and the hub is taken to be 100 mm, in order that the influence of the fixed hub on tooth-based rotation can be neglected [8].

### 6.2. Numerical analysis of gear model

Three types of finite elements have been used for meshing of gear models.

Gear models have been divided in areas and they have been meshed with elements PLANE183 [5]. These elements are defined by 8 nodes, having two degrees of freedom at each node: translations in the nodal  $x$  and  $y$  directions and are well suited to modeling irregular meshes. These elements may be used as plane elements (plane stress, plane strain and generalized plane strain) or as axisymmetric elements. These elements have plasticity, hyperelasticity, creep, stress stiffening, large deflection, and large strain capabilities (Figure 6).

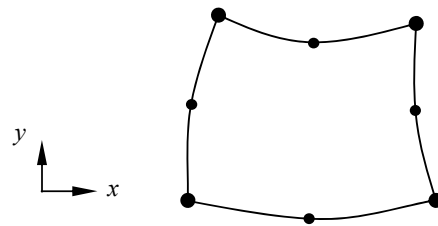


Figure 6. PLANE183 finite element

Due to contact problem analysis, the contact elements usages have proven necessary. Parts of the teeth flanks in contact have been meshed with contact elements TARGE169 and CONTA172 [5]. These parabolic elements (Figure 7) with two nodes on end and one midside node, each with two degrees of freedom (translations in the nodal  $x$  and  $y$  directions) are very suitable for analysis of problems with states of plane stress and plane strain. As they can't be used as standalone elements, they must be overlaid over existing 2D solid elements; in this case PLANE183.

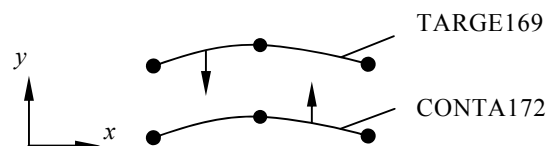


Figure 7. TARGE169 and CONTA172 contact finite element

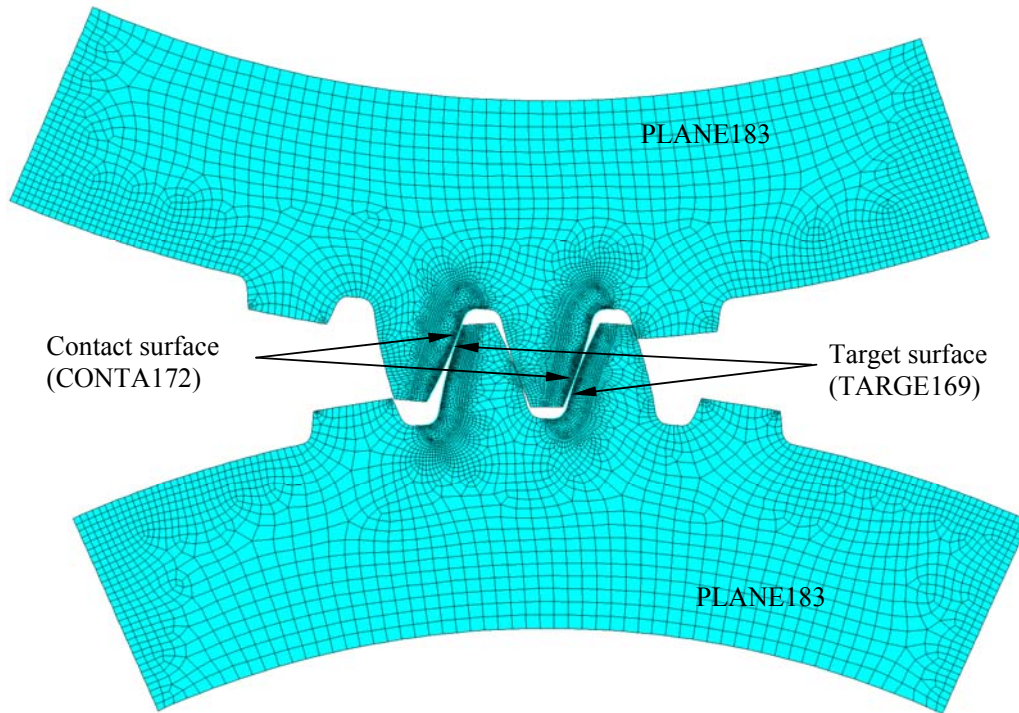


Figure 8. Meshed gear model

In order to further decrease calculation time, the finite element mesh has been adapted as well. Areas around contacting surfaces have been meshed with a larger density of finite elements mesh because these areas are crucial for the accuracy of results. Coarser finite elements have been used in areas of lesser significance, such as gear rim and segments of gear teeth that are not in contact.

The meshed gear model is shown in Figure 8.

### 6.3. Boundary conditions

The gears have been loaded by positioning mating teeth, i.e. their flanks come into contact due to inadequacy of other loading models [9]. Namely, concentrated force couldn't be applied due to the high local deformation of the material that takes place near the point of force action and this has significant influence on the results.

After positioning the mating teeth in the desired position, the boundary conditions are applied.

The wheels' nodes placed on the inner rim radius and on the ends of the rim have been constrained in the global Cartesian coordinate system  $(x, y)$  in all directions, i.e. the movements in directions of both

axes have been disabled ( $\Delta x=0$ ,  $\Delta y=0$ ). The pinions' nodes placed on the inner rim radius have been constrained in a global cylindrical coordinate system  $(r, \varphi)$  in the way of:  $\Delta r=0$ . The centre of both mentioned coordinate systems have been the centre of rotation of the pinion.

Rotation of the pinions' nodes placed on the inner rim radius around the centre of the global cylindrical coordinate system has been enabled. The angle of rotation  $\Delta\varphi$  of these nodes increased in a stepwise fashion until it resulted in a momentum of a higher than nominal torque at the pinion. The final value  $\Delta\varphi$  has been determined from the two closest rotation steps by the interpolation method.

## 7. RESULTS

Hertzian contact stresses on teeth flanks along the path of contact in the standard model have been calculated and then compared to the stresses in the modified one to present the influence of determined profile modification on Hertzian contact stresses. The results of FEM analysis for pinion and wheel are shown in Figures 9 and 10.

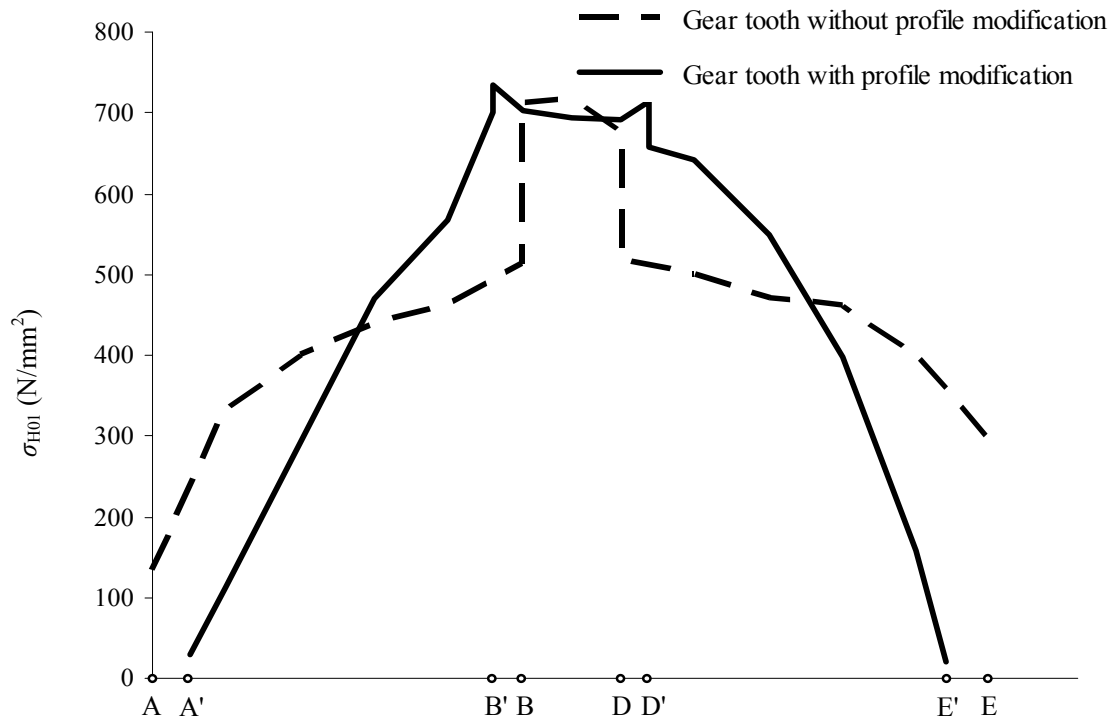


Figure 9. Hertzian contact stress for pinion ( $\sigma_{H01}$ ) for the  $i^{\text{th}}$  point of contact

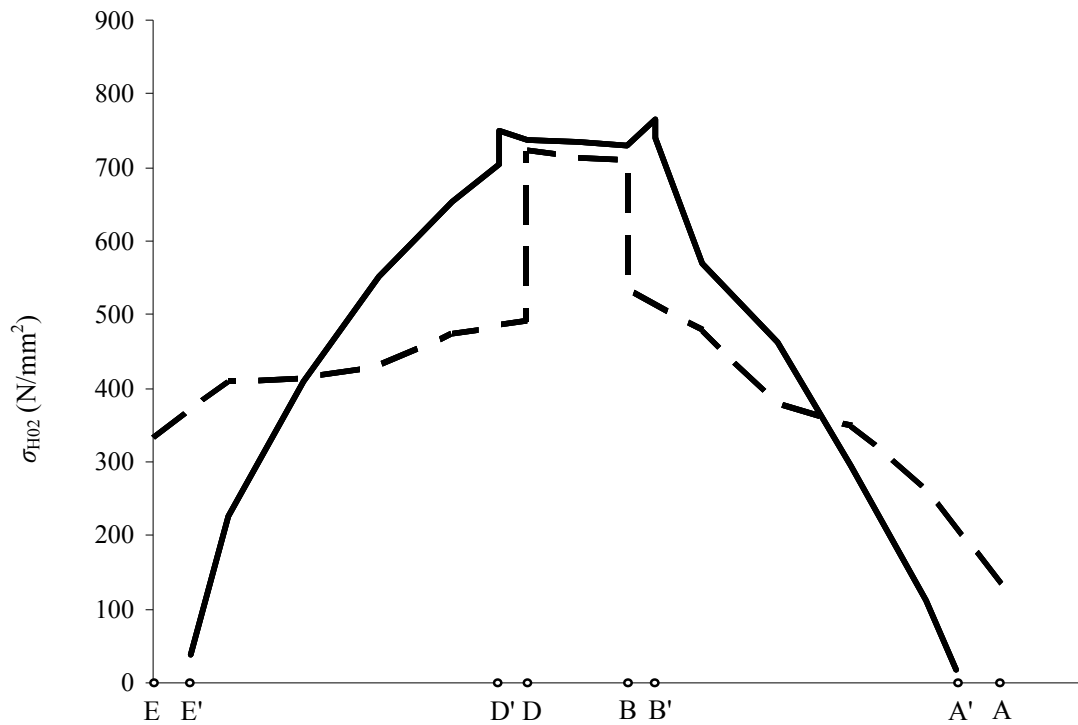


Figure 10. Hertzian contact stress for wheel ( $\sigma_{H02}$ ) for the  $i^{\text{th}}$  point of contact

For the standard unmodified model it stands that when double contact exceeds into single contact (point B on path of contact) and in reverse (point D on the path of contact), Hertzian contact stress on the tooth flank changes rapidly i.e., the wheel speed changes at two shifting points, and causes the additional dynamic load as visible in Figures 9 and 10.

Instead of the first contact between meshing gears with linear tip relief profile modification on the pinion tooth tip (point A on path of contact), it occurs lower on the tooth flank (point A' on the path of contact). The same situation appears at point E. Hertzian contact stress on tooth flank increment between points A' and B' (double contact) and decrement between points D' and E' (double contact) are almost linear. There aren't rapid stress changes at the shifting points so gears run smoother than the standard gear pair without an additional dynamic load.

The analysis also showed that the highest values of the contact stresses appear while only one tooth pair is in contact (between points B and D on the path of contact) for standard gears. The stresses show the same behavior when considering modified geometry, but the stress values are slightly higher at corresponding points B' and D' because the radius of curvature at these points are smaller than in the standard model.

### 8. CONCLUSION

The standard gear numerical model as well as the modified one have been developed and analyzed by using the finite element method. Nonlinear contact analysis has been used because it gives the most accurate results. Numerical calculation methods, such as the finite element method, provide easier stress calculations on teeth with no limits in gears' geometrical specifications and also allows determination of stress distribution on the whole path of contact.

The obtained results show that in the case of the standard unmodified model when double contact exceeds into single contact and reverse, Hertzian contact stress on tooth flank changes rapidly i.e., the wheel speed changes at two shifting points, and causes the additional dynamic load, unlike, in the case of the modified model, wheel speed does not change rapidly so there are no rapid contact stress changes at the shifting points. Also, the first contact point A' on the modified tooth profile is somewhat

lower than point A on the unmodified one. That results in stress decrease in the teeth flank at the tip area. The same situation appears at the end of contact between meshing gears with linear tip relief profile modification. This phenomenon results in such a way that the Hertzian contact stress on tooth flank increment and the decrement on double contact zones are almost linear. The disadvantage of the linear tip relief profile modification is that the increased contact stress in point B' of the modified model in relation to stress in point B on the tooth flank of the standard model, but this stress increase appears to be relatively small.

### 9. LIST OF SYMBOLS

characteristic points on path of contact	$A, A', B, B', D, D', E, E'$
auxiliary factors for calculating elastic tooth deflection	$A, B, D, E$
facewidth	$b$ , mm
half of the Hertzian contact width between the meshing teeth	$b_H$ mm
bottom clearance factor	$c^*$ , -
tip diameter	$d_a$ , mm
diameter at the beginning of tip relief profile modification	$d_k$ , mm
profile relief at tooth tip	$C_a$ , mm
modulus of elasticity	$E$ , Nmm <sup>-2</sup>
transverse load in plane of action (base tangent plane)	$F_{bt}$ , N
tool addendum factor	$h_{a0}^*$ , -
normal module	$m_n$ , mm
base radius	$r_b$ , mm
dist. between point of appl. of the force and centre of gear addendum modification	$r_p$ , mm
coefficient	$x$ , -
auxiliary angle	$\Phi$ , rad
bending arm	$y_p$ , mm
number of teeth	$z$ , -
auxiliary angle	$\alpha_b$ , °
angle of action of nominal transverse load	$\alpha_{FY}$ , °
normal pressure angle	$\alpha_n$ , °
removed material	$\Delta s$ , mm
deflection	$\delta$ , mm
bending deflection	$\delta_b$ , mm
Hertzian contact deformation	$\delta_H$ , mm
equivalent radius of the system	$\delta_{ekv}$ , mm
transverse contact ratio	$\epsilon_\alpha$ , -

Poisson's ratio	$\nu$ ,	-
roll distance	$\rho$ ,	mm
tip radius of the tool factor	$\rho_{a0}^*$ ,	-
Hertzian contact stress	$\sigma_H$ ,	$\text{Nmm}^{-2}$
nominal contact stress	$\sigma_{H0}$ ,	$\text{Nmm}^{-2}$
auxiliary angle	$\omega_b$ ,	°
index:		
pinion		1
wheel		2
i <sup>th</sup> point of contact		i

## REFERENCES

- [1] Obsieger, J.: *Some considerations to the choice of profile correction of involute gears*, STROJARSTVO, 31, p. 17-23, 1989
- [2] Terauchi, Y., Nagamura, J.: *On tooth deflection calculation and profile modification of spur gear teeth*, Intern. Symp. Gearing and Power Transmission, Proc. Vol II, pp. C-27, Tokyo, 1981, pp 159-164
- [3] Franulović, M.: *Influence of base pitch deviation on stresses in involute gearing*, Masters thesis, University of Rijeka, Faculty of Engineering, Rijeka
- [4] ISO 63361: *Calculation of load capacity of spur and helical gears*, International standard, 1996  
*Part 1: Basic principles, introduction and general influence factors*  
*Part 2: Calculation of surface durability (pitting)*  
*Part 3: Calculation of tooth bending strength*
- [5] ANSYS Structural analysis guide, Canonsburg: ANSYS Inc., 2004
- [6] Zienkewich, O.C.: *The Finite Element Method*, Mc Graw-Hill, London, 1977
- [7] Celik, M.: *Comparison of three teeth and whole body models in spur gear analysis*, Mechanism and Machine Theory 34, 2006, p. 1227-1235
- [8] Bibel, G.D.; Reddy, S.K.; Savage, M. & Handsuch, G.F.: *Effects of rim thickness on spur gear bending stress*, NASA Technical Memorandum 104388, Technical Report 91-C-015, Houston, 1991
- [9] Basan, R.; Franulović, M. & Križan, B.: *Numerical model and procedure for determination of stresses in spur gears teeth flanks*, Proceedings of XII International conference on mechanical engineering, Starek, L. & Hučko, B. (Ed.), Bratislava, 2008

Received: 28.03.2011

Accepted: 16.05.2011.

Original scientific paper

Authors' address

Kristina Marković

Marina Franulović

University of Rijeka

Faculty of engineering

Vukovarska 58

51000 Rijeka

CROATIA

[kristina@riteh.hr](mailto:kristina@riteh.hr)

[marina.franulovic@riteh.hr](mailto:marina.franulovic@riteh.hr)